

# Ising Formulation for OTFS Maximum Likelihood Channel Estimation

Thomas Trieu

*Department of Electrical and Computer Engineering, Rutgers University–New Brunswick, NJ, USA*

Emails: thomas.t.trieu@rutgers.edu

**Abstract**—Orthogonal Time Frequency Space (OTFS) modulation offers superior resilience to high-mobility and severe Doppler spread environments, making it highly attractive for complex channels such as underwater acoustic communications. However, achieving optimal Maximum Likelihood Channel Estimation (MLCE) in OTFS remains an NP-hard problem due to the discrete nature of the Delay-Doppler (DD) grid. This work addresses the high computational burden by reformulating the OTFS MLCE problem into a Quadratic Unconstrained Binary Optimization (QUBO) model, which is then mapped to the Ising Hamiltonian. The complex-valued, continuous ML objective is converted into a fully binary form using a real-valued decomposition and a novel additive offset quantization scheme to accurately encode complex channel gains. The resulting Ising problem is solved using physics-inspired optimization algorithms, specifically Simulated Annealing (SA) and Parallel Tempering (PT), implemented via the open-source PySA solver. Performance evaluation demonstrates a strong proof-of-concept, achieving high channel estimation accuracy across various noise levels, with the Normalized Mean Squared Error (NMSE) quantified against optimal solver parameters. This Ising formulation not only provides an energy-based, optimal solution path for OTFS MLCE but also establishes direct compatibility with emerging quantum annealing platforms for potential future quantum acceleration.

**Index Terms**—OTFS, Channel Estimation, Maximum Likelihood, Ising Model, QUBO, Quantum Annealing, Simulated Annealing, Underwater Acoustic Communications, Sparse Recovery

## I. INTRODUCTION

Underwater wireless communication systems enable many critical applications including scientific expeditions, environmental monitoring, and military deployments [1]. Because radio and optical waves attenuate and scatter underwater, mechanical waves become the more practical option for long distances. However, the underwater acoustic channel has unique characteristics such as low bandwidth, high propagation delay, multi-path, and fading. Due to its dynamic nature and harsh conditions, minimizing the size, weight, power usage, and cost of underwater modems while simultaneously maximizing the bandwidth, bitrate, and range is crucial for implementing practical underwater acoustic communication systems [2]. Various categories of modulation techniques have been researched in order to improve performance in the underwater acoustic channel, including single carrier modulation (SCM), multicarrier modulation (MCM), spread spectrum (SS), spatial modulation (SM), and hybrid carrier modulation (HCM) [3]. This paper focuses on orthogonal time frequency space (OTFS) [4], an extension of OFDM [5]. OTFS modulation in the delay-

Doppler (DD) domain enables superior robustness in high-mobility scenarios, but its additional dual transform operations on top of orthogonal frequency division multiplexing (OFDM) introduce significant computational complexity [4]. OTFS has also recently been proven to be fundamentally equivalent to orthogonal signal division multiplexing (OSDM) in [6], so any related works that strive to improve the complexity of either of them will be analyzed in parallel. OTFS modulation introduces a superior peak-to-average power ratio (PAPR), Doppler resilience, joint channel estimation (CE) capabilities, and timing robustness over OFDM. This makes OTFS very attractive for implementation in underwater acoustic communications.

**Motivations:** OTFS modulation introduces a superior peak-to-average power ratio (PAPR), Doppler resilience, joint channel estimation (CE) capabilities, and timing robustness over OFDM. This makes OTFS very attractive for implementation in underwater acoustic communications. However, prior work either yields high computational complexity, requires matrix inversion, does not fully eliminate inter-path interference (IPI), or cannot handle dynamic scenarios well [7]. Realistically estimating the underwater channel brings many challenges. Because of the low speed of sound, the propagation delay is five orders of magnitude higher than in electro-magnetic terrestrial channels. This often leads to the underwater channel being overspread, meaning the characteristics of the channel change while symbols are still being transmitted through the channel. An overspread channel results in aliased delays in the DD domain due to OTFS modulo operation [8]. Additionally, in practice, path delays may not be exact integer multiples of the delay resolution, nor are Doppler shifts exact multiples of the Doppler resolution. When the multi-path components do not align with the DD grid points, the energy leakage that destroys DD domain sparsity and introduces severe IPI heavily degrades channel estimation performance [7]. This breaks sparsity assumptions underlying prior methods like orthogonal matching pursuit (OMP) [9]. Traditional channel estimation methods fail under such conditions, emphasizing the need for a more thorough exploration of advanced channel estimation methods. Because the underwater acoustic channel is very dynamic and complex, many efforts have been made to improve OTFS CE by designing more advanced CE techniques or lower complexity algorithms [10]. The trade off between lowering the bit error rate (BER) and lowering the computational complexity is very prominent.

Over the past few years, there has been a noticeable surge of

interest in alternative computing approaches with the goal of reducing computational complexity while maintaining state-of-the-art accuracy by relating optimization convergence to physics principles. Alternative computing such as quantum annealing is gaining traction especially as quantum computing is gaining public interest. They are mainly directed toward equalization and maximum-likelihood detection which is the main cause of computational latency in wireless communications [11, 12, 13]. These approaches have potential for enabling optimal solutions for NP-hard optimization problems, and discrete combinatorial problems like OTFS MLCE can be mapped to an Ising formulation to be solved using quantum annealing [14].

**Contributions:** This work proposes the design and implementation of an Ising formulation for OTFS MLCE that enables the use of Ising solvers for efficient optimization. Its performance is evaluated through simple channel simulations using PySA, an open-source optimization problem solver developed by NASA [15], and the normalized mean squared error (NMSE) and runtime is analyzed under various solver and noise parameters. This formulation ultimately opens up the opportunity for quantum acceleration through quantum annealing, which can reduce computational complexity while maintaining optimal channel estimation accuracy.

## II. BACKGROUND

This section introduces background knowledge explaining pilot-based OTFS channel estimation and the maximum likelihood channel estimation problem, simulated annealing (SA), parallel tempering (PT), and then related work on channel estimation as well as alternative computing approaches that are used for other applications such as equalization.

### A. Maximum Likelihood (ML) Channel Estimation

In typical OFDM pilot-based channel estimation [16], a known pilot  $X_{tf}$  is converted to the time domain through the Inverse Fast Fourier Transform (IFFT) and the signal  $x(t)$  is transmitted through the channel  $H$ . When the signal  $y(t)$  is received and converted to the frequency domain through the Fast Fourier Transform (FFT), the channel can now be estimated. As shown in Fig. 1, OTFS takes the modulation a step further and adds an additional layer of transforms on top of OFDM. The IFFT becomes the Heisenberg Transform, the FFT becomes the Wigner Transform, and the Inverse Symplectic Finite Fourier Transform (ISFFT) and Symplectic Finite Fourier Transform (SFFT) are placed around the OFDM transforms [4]. The pilot is now inserted in the delay-Doppler (DD) domain and goes through two transforms before being transmitted.

Maximum Likelihood (ML) estimation [17] in the context of OTFS seeks the channel parameters

$$\mathbf{h} = (\alpha_l, \tau_l, \nu_l)_{l=1}^L \quad (1)$$

that maximizes the likelihood of observing the received signal  $y$  given the transmitted signal  $x$ , where  $\alpha_l$  is the complex gain of the  $l$ -th path,  $\tau_l$  is the delay of the  $l$ -th path, and  $\nu_l$

is the Doppler shift of the  $l$ -th path. In OTFS, complex gains are continuous values while delays and Dopplers are discrete values. Because the DD grid in OTFS has a discrete number of taps, iterating through the delay and Doppler taps becomes a discrete combinatorial optimization problem, making the maximum likelihood estimation NP-hard. In a linear system

$$\mathbf{y} = \mathbf{H}\mathbf{x} + \mathbf{n}, \quad (2)$$

maximizing this likelihood is equivalent to minimizing the cost function:

$$E(\mathbf{H}) = \|\mathbf{y} - \mathbf{H}\mathbf{x}\|^2, \quad (3)$$

and the ML estimate of the channel is obtained as

$$\hat{\mathbf{H}}_{\text{ML}} = \arg \min_{\mathbf{H}} E(\mathbf{H}). \quad (4)$$

However, when the channel exhibits nonlinearities, time variation, or multi-path/Doppler effects,  $E(\mathbf{H})$  becomes non-convex and may contain numerous local minima. This motivates the use of global optimization methods like SA and PT to approximate  $\hat{\mathbf{H}}_{\text{ML}}$ .

### B. Simulated Annealing

Simulated Annealing (SA) is a classical stochastic optimization algorithm inspired by the annealing process in metallurgy, where materials are heated and slowly cooled to reach a state of minimum energy. Introduced in [18], it is designed to find near-global optima for complex cost functions where gradient-based methods may get trapped in local minima. Simulated Annealing is widely used in combinatorial optimization and continuous parameter estimation problems where the objective function is non-convex or discontinuous. The method operates by drawing an analogy between the optimization problem and a physical system characterized by an energy objective function  $H(\mathbf{s})$  (or Hamiltonian) of Ising spin problems, often modeled as a quadratic cost function:

$$H(\mathbf{s}) = \sum_{ij} J_{ij} s_i s_j + \sum_i h_i s_i, \quad (5)$$

where each spin  $s_i \in \{-1, +1\}$ ,  $J_{ij}$  denotes the correlation preference between two spins  $i$  and  $j$ , and  $h_i$  is a magnetic field acting on spin  $i$ . SA explores the solution space by randomly and slightly changing the current solution and accepting or rejecting the new state according to a Boltzmann probability distribution:

$$P(\mathbf{s}') \propto \exp \left( -\frac{E(\mathbf{s}')}{k_B T} \right), \quad (6)$$

where  $T$  is the temperature and  $k_B$  is the Boltzmann constant (often set to 1 in normalized systems). A new configuration  $\mathbf{s}'$  is accepted with probability

$$P_{\text{accept}} = \begin{cases} 1, & \text{if } \Delta E \leq 0, \\ \exp \left( -\frac{\Delta E}{T} \right), & \text{if } \Delta E > 0, \end{cases} \quad (7)$$

where  $\Delta E = E(\mathbf{s}') - E(\mathbf{s})$ . The temperature parameter  $T$  gradually decreases according to a cooling schedule (exponential or logarithmic). At high temperatures, the algorithm accepts

## Delay-Doppler Domain (OTFS)

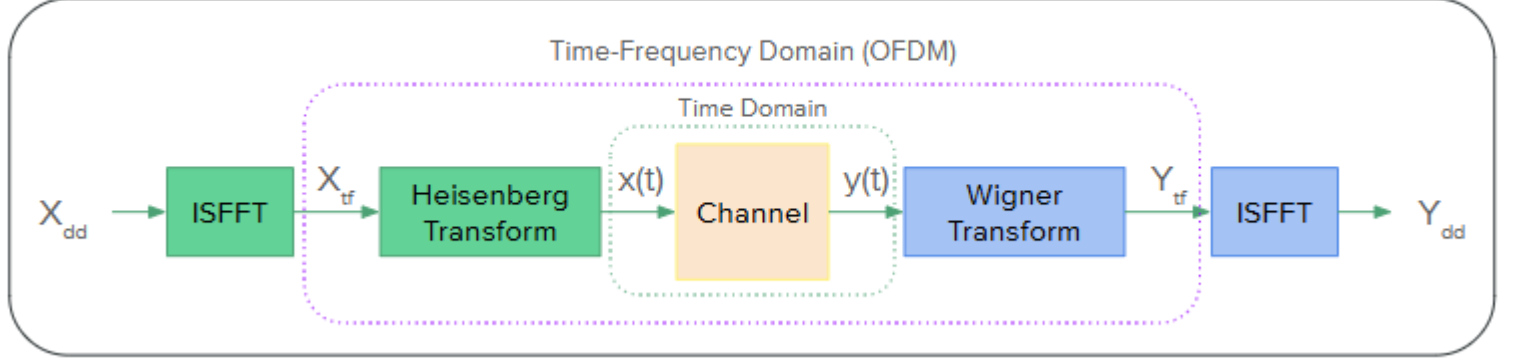


Fig. 1. Diagram of OTFS-based communication.

worse solutions to encourage exploration, and as temperature decreases, it focuses more on exploitation, ideally converging to the global minima.

### C. Parallel Tempering

Parallel Tempering (PT), introduced in [19] as Replica Exchange Monte Carlo, is an extension of simulated annealing designed to improve convergence and escape local minima by running multiple Markov chains at different temperatures in parallel.  $N$  replicas of the system are simulated simultaneously at temperatures  $T_1 < T_2 < \dots < T_N$ . Similarly to simulated annealing, high-temperature replicas explore the solution space freely, whereas low-temperature replicas focus on refinement. For two neighboring replicas  $i$  and  $j$  with inverse temperatures  $\beta_i = 1/T_i$  and  $\beta_j = 1/T_j$ , a configuration exchange is proposed and accepted with probability:

$$P_{\text{swap}} = \min(1, \exp[(\beta_i - \beta_j)(E_i - E_j)]). \quad (8)$$

This exchange allows low-temperature chains to escape local minima by occasionally swapping with higher-temperature chains that can explore more broadly.

### D. Related Work

The 3D-Structured Orthogonal Matching Pursuit (3D-SOMP) in [20] addresses the estimation of the downlink channel in OTFS by formulating it as a sparse signal recovery problem. This approach efficiently exploits the multidimensional sparsity and outperforms the standard orthogonal matching pursuit (OMP) in both the accuracy of the channel state information (CSI) and the reduced pilot overhead. However, involving iterative multidimensional searches and transformations would be computationally demanding for real-time large-scale systems. In [21], a channel estimation technique that embeds the pilot, guard, and data symbols directly into the delay-Doppler grid of each OTFS frame is proposed. It enables channel estimation and data detection within the same frame, minimizing latency and outdated estimates, but requires a high pilot SNR for ideal-like performance—not ideal for low-power underwater acoustic modems. The approach in [22]

demonstrates robustness to channel variations by proposing an improved sparse Bayesian learning (I-SBL) algorithm although it requires significant computational resources for real-time implementation. In [23], OSDM is integrated with an orthogonal multiple access based on the Basis Expansion Model (BEM), providing significant power efficiency and Doppler resilience (D-OSDM) over traditional OFDM and OSDM. This imposes an increased computational load at the receiver, which is challenging for resource-constrained modems. The Carrier Frequency Offset Compensation for OSDM (CFO-C-OSDM) in [24] achieves lower uncoded and coded BERs than D-OSDM across CFO ranges up to  $\pm 200$  Hz under SNRs (signal-to-noise ratios) of 10-20 dB. However, the advanced estimation algorithm and additional matrix operations increase computational complexity. There have also been efforts to implement OTFS for underwater acoustic communications in [25] and [26] after OSDM and OTFS were proven to be fundamentally equivalent. The multiple-step approach in [25] offers consistent BER advantages over OFDM but introduces processing latency, and [26] achieves high channel estimation accuracy at the expense of increased computational demands through the use of large-scale matrix operations and spline interpolations. The message-passing-based low-complexity bidirectional channel estimation algorithm (LCE-MP) in [27] superimposes training sequences on data symbols for enhanced channel tracking without significant spectrum overhead, enabling global channel estimation through the exploitation of correlations between adjacent segments. This is done under the assumption that the underwater acoustic channel does not change abruptly, which may not hold in highly dynamic environments. The first real-time OSDM modem implementation in [28] demonstrates reliable, low-latency underwater acoustic communication with multi-kilometer ranges. Still, its heterogeneous digital signal processing (DSP) and field-programmable gate array (FPGA) hardware increases system complexity, size, and power draw, while its limited Doppler tolerance causes BER to increase at frequency offsets of more than  $\pm 5$  Hz.

Quantum annealing has been used for ML detection in large MIMO systems in [29], and reverse annealing for ML detection in [30]. The ParaMax Ising Solver (PMIS) in [31] features an SA-based parallel tempering algorithm that is highly tailored to optimize the Ising model for OFDM Maximum Likelihood MIMO detection. It is a classical physics-inspired design, compared to the quantum annealing version in [29], that can be run on generic classical hardware. Instead of ML detection, an Ising model for OTFS MLCE is proposed.

### III. PROPOSED SOLUTION

In this section, I will go through reformulating OTFS ML channel estimation equation into the Ising model.

#### A. Channel Space and Variable Discretization

In OTFS, the physical channel can be considered as a sum of L propagation paths:

$$h(\tau, \nu) = \sum_{i=1}^L \alpha_i \cdot \delta(\tau - \tau_i) \delta(\nu - \nu_i). \quad (9)$$

$\alpha_i$  is the complex path gain and  $(\tau_i, \nu_i)$  is the delay/Doppler shift. These are the parameters that will be estimated. The delay-Doppler grid can be discretized, and the parameter vector  $h$  becomes a sparse vector of possible taps where only a few entries are non-zero. Most grid points have zero response, and a few have strong paths. In a grid of  $M = 4$  delays and  $N = 4$  Dopplers (can be scaled for fractional delays and Dopplers), there are  $MN = 16$  possible taps. However, for each tap, there is a complex gain. The complex gain is a continuous parameter, but mapping to the Ising form requires discrete variables. This introduces quantization error that would be significant if the number of bits used to discretize the complex gain is not large enough. I used  $n_{bits} = 4$ , and the performance of this decision is evaluated in section IV. For each possible change in parameters, introduce a binary variable  $q_k \in \{0, 1\}$  where  $k$  is the index for the variable in the configuration, or state  $q$ , and 0 and 1 is active and inactive, respectively. Additionally, because the gain is complex, there are real and imaginary parts. So for each gain, we need to have two sets of quantizations. This complicates our ML objective because the Ising model can only accept a real-valued problem. Given the pilot:

$$\mathbf{y} = \Phi \mathbf{h} + \mathbf{w}, \quad (10)$$

- $\mathbf{y} \in \mathbb{C}^{MN \times 1}$ : Received signal vector
- $\Phi \in \mathbb{C}^{MN \times MN}$ : The known pilot matrix (each column is a DD grid point's contribution)
- $\mathbf{h} \in \mathbb{C}^{MN \times 1}$ : The channel coefficients to estimate
- $\mathbf{w}$ : Gaussian noise

We can concatenate the complex part of  $\mathbf{h}$  and  $\mathbf{y}$  and append it to the end of the real part. This doubles the number of variables in a state. For the pilot matrix:

$$\Phi_{\text{real}} = \begin{bmatrix} \text{Re}(\Phi) & -\text{Im}(\Phi) \\ \text{Im}(\Phi) & \text{Re}(\Phi) \end{bmatrix}. \quad (11)$$

The real-valued conversion takes us from (10) to

$$\mathbf{y}_{\text{real}} = \Phi_{\text{real}} \mathbf{h}_{\text{real}} + \mathbf{w}. \quad (12)$$

- $\mathbf{y}_{\text{real}} \in \mathbb{C}^{2MN \times 1}$ : Received signal vector
- $\Phi_{\text{real}} \in \mathbb{C}^{2MN \times 2MN}$ : The known pilot matrix (each column is a DD grid point's contribution)
- $\mathbf{h}_{\text{real}} \in \mathbb{C}^{2MN \times 1}$ : The channel coefficients to estimate
- $\mathbf{w}$ : Gaussian noise

Thus, the total number of variables in a state  $q$  is  $n_{vars} = 2MNn_{bits}$ . This sets up the complex estimation problem for binary optimization where every possible solution (which variables are active/inactive) is a binary vector  $\mathbf{q}$ . The next step is to map the  $n_{bits}$  to the gain values while accounting for negative gains. This is done by substituting  $\mathbf{h}_{\text{real}}$  using a quantization matrix  $\mathbf{T}$ , binary variables  $q \in \{0, 1\}^{n_{vars}}$ , and an additive offset  $\mathbf{b}_{\text{offset}}$  to handle both positive and negative channel gains:

$$\mathbf{h}_{\text{real}} = \mathbf{T}q - \mathbf{b}_{\text{offset}} \quad (13)$$

$$\mathbf{b}_{\text{offset}} = [\alpha_{\max} \quad \alpha_{\max} \quad \dots \quad \alpha_{\max}]^T, \text{ Shape: } 2MN \times 1$$

$$\mathbf{T} = \mathbf{I}_{n_{vars}} \otimes \mathbf{v}_{\text{bits}}, \text{ Shape: } 2MN \times n_{vars}$$

$$\mathbf{v}_{\text{bits}} = [2 \cdot \alpha_{\max} \cdot 2^{-1} \quad 2 \cdot \alpha_{\max} \cdot 2^{-2} \quad \dots \quad 2 \cdot \alpha_{\max} \cdot 2^{-n_{bits}}]$$

where  $\otimes$  denotes the Kronecker product. We also need to substitute  $\mathbf{y}_{\text{real}}$  with a modified version:

$$\mathbf{y}_{\text{mod}} = \mathbf{y}_{\text{real}} + \Phi_{\text{real}} \mathbf{b}_{\text{offset}}, \text{ Shape: } 2MN \times 1 \quad (14)$$

#### B. ML Objective to Ising Formulation

The objective is to best explain the received pilot signals  $y$  given the guess for the channel support. With a known pilot matrix  $\Phi_{\text{real}}$  and the channel tap vector  $\mathbf{h}_{\text{real}}$  constructed from the binary variables  $q_k$ , we have the objective function:

$$\hat{\mathbf{h}}_{\text{real}}(q)_{\text{ML}} = \arg \min_h \|\mathbf{y}_{\text{mod}} - \Phi_{\text{real}} \mathbf{h}_{\text{real}}(q)\|^2 \quad (15)$$

with  $\mathbf{h}_{\text{real}}(q)$  expressing the channel as a sum of activated taps. When the ML objective is expanded, only terms involving  $\mathbf{q}$  matter, and the cost becomes quadratic in  $\mathbf{q}$ , leading to the quadratic unconstrained binary optimization (QUBO) form:

$$E(\mathbf{x}) = \mathbf{q}^T \mathbf{Q} \mathbf{q} + \mathbf{L}^T \mathbf{q} \quad (16)$$

$$\mathbf{A} = \Phi_{\text{real}} \mathbf{T}, \text{ Shape: } 2MN \times n_{vars}$$

$$\mathbf{Q} = \mathbf{A}^T \mathbf{A}, \text{ Shape: } n_{vars} \times n_{vars}$$

$$\mathbf{L} = -2(\mathbf{y}_{\text{mod}})^T \mathbf{A}, \text{ Shape: } n_{vars} \times 1$$

The Ising model uses *spins* instead of *bits*, so the spin  $s_k \in \{-1, 1\}$  for state  $s$  would be used instead of  $q_k$  and  $q$ . The solver initializes all the spins at 1 instead of 0, and the solver will randomly flip one spin at a time based on the probabilities in (7) and (8), favoring a sparse channel in the DD domain. To convert the QUBO problem to the Ising Hamiltonian, we use the substitution  $q_k = \frac{1-s_k}{2}$ :

$$\mathcal{H}(s) = \sum_{i < j} J_{ij} s_i s_j + \sum_i h_i s_i \quad (17)$$

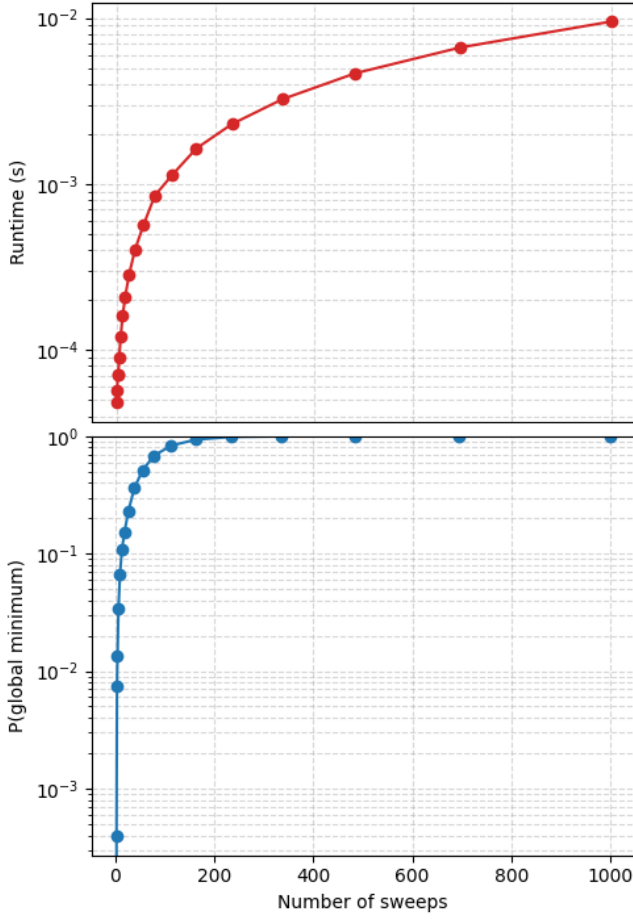


Fig. 2. Sweep analysis at  $n_{\text{reads}} = 5000$  for each data point to determine optimal number of sweeps.

$$J_{ij} = \frac{1}{4}Q_{ij}, \text{ for } i \neq j$$

$$h_i = \frac{1}{2}L_i + \frac{1}{4} \sum_{j=1}^{n_{\text{vars}}} Q_{ij}$$

We now have the Ising coupling matrix  $\mathbf{J}$  and the Ising local field vector  $\mathbf{h}$ . These are the two variables that will be inputs for the PySA solver. The output of the solver will be the state  $s$  with the lowest energy in that run.

#### IV. PERFORMANCE EVALUATION

In this section, the performance of the Ising-based OTFS MLCE will be discussed. With the output  $s$  from the PySA solver, we demap it to get the estimated channel that we then compare to the true channel that was pseudo-randomly generated and used to simulate the system. The parameter decisions will also be discussed in detail.

**Metropolis Sweeps:** Increasing the number of Metropolis sweeps gives more time for the Ising solver to reach the global minimum in the optimization. This is because the range of temperature is static while the increasing number

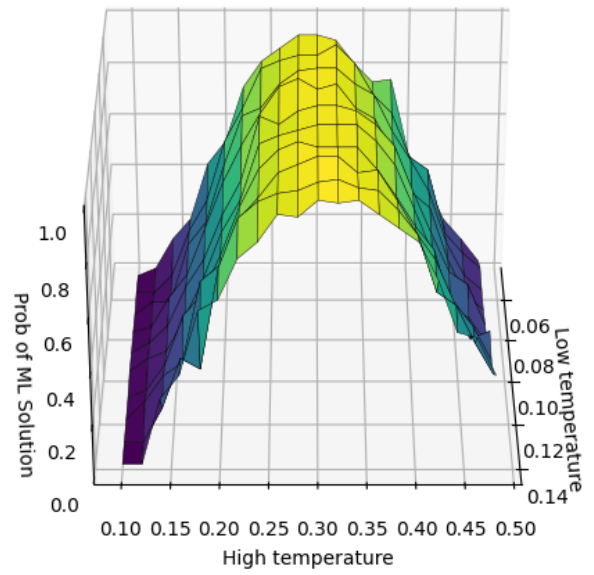


Fig. 3. Phase diagram at  $n_{\text{reads}} = 100$  for each data point to visualize optimal temperature range.

of sweeps means the SA process "cools" the system slower. A sweep analysis was done to visualize and determine the optimal number of Metropolis sweeps that would maximize the probability of reaching the global minimum while keeping a tractable runtime. As shown in Fig. 2,  $n_{\text{sweeps}} = 100$  provides a very high probability of reaching the global minimum while keeping runtime around 1 millisecond. The number of replicas that are used is  $n_{\text{replicas}} = 2$  to keep computational complexity as low as possible while taking advantage of PT.

**Temperature Range:** The temperature range for the SA process determines the behavior of the system when encountering local minima. A temperature phase diagram was made in Fig. 3 to visualize how different temperature ranges would affect the probability of reaching the global minimum. Based on the phase diagram, a strict upper bound  $T_{\text{high}} = 0.3$  appears to be optimal, while the lower bound is very lenient. I chose  $T_{\text{low}} = 0.1$  for the lower bound in my simulation runs.

**Estimation Accuracy:** The performance of the Ising-based OTFS MLCE was evaluated at increasing levels of simulated AWGN. As shown in Fig. 4, the normalized mean squared error (NMSE) sharply increases as SNR drops below 10 dB. This is likely due to the noise making the global minimum more shallow, causing the solver to treat it as a local minimum.

#### V. CONCLUSIONS

This work successfully proposed and implemented a novel transformation of the OTFS MLCE problem into the Ising Hamiltonian. By employing a real-valued matrix decomposition and an additive offset quantization scheme, we overcame the challenge of mapping continuous, complex-valued channel gains (including negative values) into the required binary spin

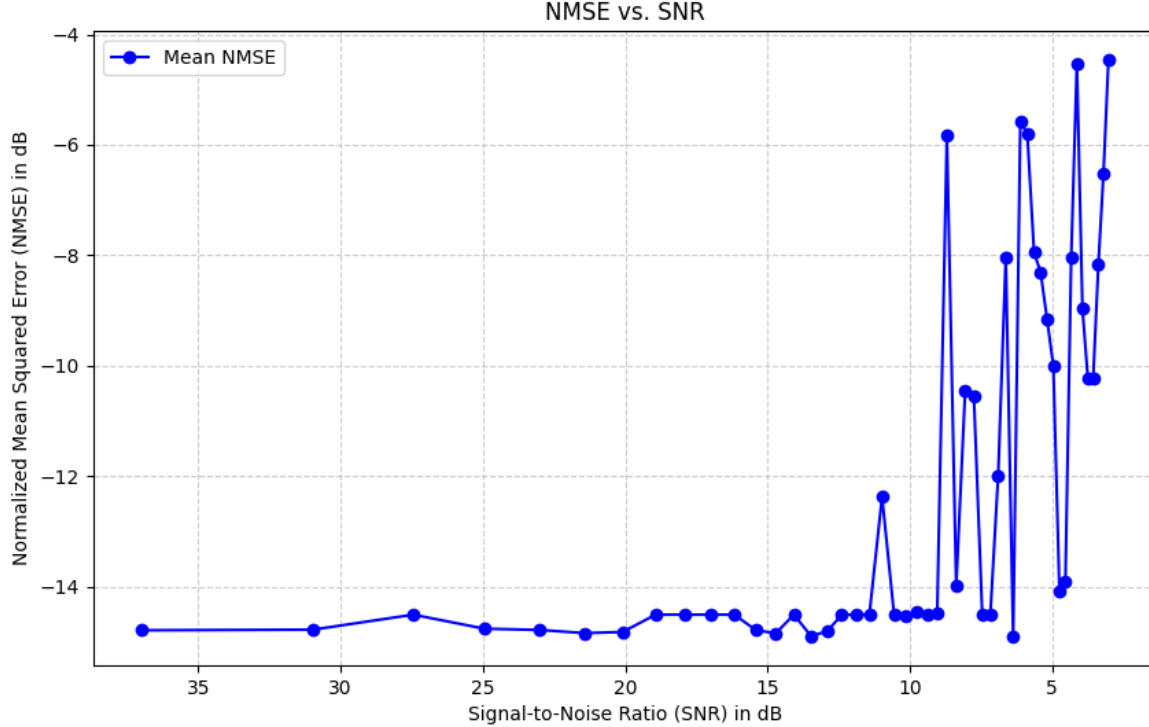


Fig. 4. Estimation accuracy as simulated noise increases.

variables. This formulation enables the use of efficient physics-inspired optimization methods, such as SA and PT, using the PySA solver. The performance evaluation provided a crucial proof-of-concept, demonstrating that the Ising formulation can accurately estimate the sparse DD channel, with the NMSE performance bounded by the increasing noise floor. Optimal solver parameters were also established, involving a low-complexity sweep count and a stable temperature range, necessary for practical implementation. Crucially, this work is not limited to classical SA/PT solvers. The resulting Ising formulation, defined by the coupling matrix  $J$  and local field vector  $\mathbf{h}$ , is directly compatible with quantum annealing hardware (e.g., D-Wave systems) and other emerging quantum-inspired accelerators. This capability provides a clear path toward potential quantum acceleration, promising a significant reduction in computational complexity for achieving optimal MLCE solutions in future large-scale OTFS systems. While the simulation successfully demonstrates the high accuracy of the channel estimation problem, a full performance assessment requires further study. Future work should focus on three primary areas: first, evaluating the end-to-end equalization performance and BER achieved by the estimated channel to assess the practical impact on data throughput; second, testing the Ising model's performance in a more realistic, non-grid-aligned channel environment where IPI and fractional Doppler effects degrade sparsity; and third, comparing the NMSE and

runtime against established benchmarks like OMP and other state-of-the-art algorithms across a wider range of mobility and channel conditions.

## REFERENCES

- [1] Dario Pompili and Ian F. Akyildiz. “Overview of networking protocols for underwater wireless communications”. In: *IEEE Communications Magazine* 47.1 (2009), pp. 97–102. DOI: 10.1109/MCOM.2009.4752684.
- [2] Filippo Campagnaro et al. “Affordable underwater acoustic modems and their application in everyday life: a complete overview”. In: *Proceedings of the 17th International Conference on Underwater Networks & Systems*. WUWNet ’23. Shenzhen, China: Association for Computing Machinery, 2024. ISBN: 9798400716744. DOI: 10.1145/3631726.3631734. URL: <https://doi.org/10.1145/3631726.3631734>.
- [3] Muhammad Haziq et al. “Modulation Techniques for Underwater Acoustic Communication: A Comprehensive Survey”. In: *IEEE Access* 13 (2025), pp. 150715–150755. DOI: 10.1109/ACCESS.2025.3601799.
- [4] R. Hadani et al. “Orthogonal Time Frequency Space Modulation”. In: *2017 IEEE Wireless Communications and Networking Conference (WCNC)*. 2017, pp. 1–6. DOI: 10.1109/WCNC.2017.7925924.

- [5] Lie-Liang Yang. “Orthogonal Time-Frequency-Space (OTFS) and Related Signaling”. In: *arXiv preprint arXiv:2401.13790* (2024).
- [6] Ids van der Werf et al. “On the equivalence of OSDM and OTFS”. In: *Signal Processing* 214 (2024), p. 109254. ISSN: 0165-1684. DOI: <https://doi.org/10.1016/j.sigpro.2023.109254>. URL: <https://www.sciencedirect.com/science/article/pii/S0165168423003286>.
- [7] Guangyu Lei et al. *Low-Complexity Channel Estimation in OTFS Systems with Fractional Effects*. 2025. arXiv: 2505.06248 [eess.SP]. URL: <https://arxiv.org/abs/2505.06248>.
- [8] Preety Priya, Yi Hong, and Emanuele Viterbo. “OTFS Channel Estimation and Detection for Channels With Very Large Delay Spread”. In: *IEEE Transactions on Wireless Communications* 23.9 (2024), pp. 11920–11930. DOI: 10.1109/TWC.2024.3386160.
- [9] Rabah Ouchikh et al. “Sparse channel estimation algorithms for OTFS system”. In: *IET Communications* 16.18 (2022), pp. 2158–2170. DOI: <https://doi.org/10.1049/cmu2.12469>. eprint: <https://ietresearch.onlinelibrary.wiley.com/doi/pdf/10.1049/cmu2.12469>. URL: <https://ietresearch.onlinelibrary.wiley.com/doi/abs/10.1049/cmu2.12469>.
- [10] Emir Aslandogan et al. *A Comprehensive Survey of Channel Estimation Techniques for OTFS in 6G and Beyond Wireless Networks*. 2025. arXiv: 2512.13032 [eess.SP]. URL: <https://arxiv.org/abs/2512.13032>.
- [11] Edward Farhi, Jeffrey Goldstone, and Sam Gutmann. *A Quantum Approximate Optimization Algorithm*. 2014. arXiv: 1411.4028 [quant-ph]. URL: <https://arxiv.org/abs/1411.4028>.
- [12] Stuart Hadfield et al. “From the Quantum Approximate Optimization Algorithm to a Quantum Alternating Operator Ansatz”. In: *Algorithms* 12.2 (2019). ISSN: 1999-4893. DOI: 10.3390/a12020034. URL: <https://www.mdpi.com/1999-4893/12/2/34>.
- [13] Minsung Kim. “Quantum and Quantum-Inspired Computation for NextG MIMO Wireless Communications”. In: *Proceedings of the 22nd Annual International Conference on Mobile Systems, Applications and Services*. MOBISYS ’24. Minato-ku, Tokyo, Japan: Association for Computing Machinery, 2024, pp. 756–757. ISBN: 9798400705816. DOI: 10.1145/3643832.3661388. URL: <https://doi.org/10.1145/3643832.3661388>.
- [14] Andrew Lucas. “Ising formulations of many NP problems”. In: *Frontiers in Physics* Volume 2 - 2014 (2014). ISSN: 2296-424X. DOI: 10.3389/fphy.2014.00005. URL: <https://www.frontiersin.org/journals/physics/articles/10.3389/fphy.2014.00005>.
- [15] PA Lott et al. “QuAIL Tools for Benchmarking, Analysis and Quantum Algorithm Development”. In: *Adiabatic Quantum Computing 2023*. 2023.
- [16] S. Coleri et al. “Channel estimation techniques based on pilot arrangement in OFDM systems”. In: *IEEE Transactions on Broadcasting* 48.3 (2002), pp. 223–229. DOI: 10.1109/TBC.2002.804034.
- [17] Pei Chen and H. Kobayashi. “Maximum likelihood channel estimation and signal detection for OFDM systems”. In: *2002 IEEE International Conference on Communications. Conference Proceedings. ICC 2002 (Cat. No.02CH37333)*. Vol. 3. 2002, 1640–1645 vol.3. DOI: 10.1109/ICC.2002.997127.
- [18] Nicholas Metropolis and S. Ulam. “The Monte Carlo Method”. In: *Journal of the American Statistical Association* 44.247 (1949). PMID: 18139350, pp. 335–341. DOI: 10.1080/01621459.1949.10483310. eprint: <https://www.tandfonline.com/doi/pdf/10.1080/01621459.1949.10483310>. URL: <https://www.tandfonline.com/doi/abs/10.1080/01621459.1949.10483310>.
- [19] Robert Swendsen and Jian-Sheng Wang. “Replica Monte Carlo Simulation of Spin-Glasses”. In: *Physical review letters* 57 (Dec. 1986), pp. 2607–2609. DOI: 10.1103/PhysRevLett.57.2607.
- [20] Wenqian Shen et al. “Channel Estimation for Orthogonal Time Frequency Space (OTFS) Massive MIMO”. In: *IEEE Transactions on Signal Processing* 67.16 (2019), pp. 4204–4217. DOI: 10.1109/TSP.2019.2919411.
- [21] P. Raviteja, Khoa T. Phan, and Yi Hong. “Embedded Pilot-Aided Channel Estimation for OTFS in Delay-Doppler Channels”. In: *IEEE Transactions on Vehicular Technology* 68.5 (2019), pp. 4906–4917. DOI: 10.1109/TVT.2019.2906357.
- [22] Xiangzhao Qin, Fengzhong Qu, and Yahong Rosa Zheng. “Bayesian Iterative Channel Estimation and Turbo Equalization for Multiple-Input–Multiple-Output Underwater Acoustic Communications”. In: *IEEE Journal of Oceanic Engineering* 46.1 (2021), pp. 326–337. DOI: 10.1109/JOE.2019.2956299.
- [23] Tadashi Ebihara and Geert Leus. “Doppler-Resilient Orthogonal Signal-Division Multiplexing for Underwater Acoustic Communication”. In: *IEEE Journal of Oceanic Engineering* 41.2 (2016), pp. 408–427. DOI: 10.1109/JOE.2015.2454411.
- [24] Zhuoran Qi et al. “Carrier Frequency Offset Compensation for OSDM in Underwater Acoustic Communications: Theory and Experiments Using a Vector MIMO Modem”. In: *2025 59th Annual Conference on Information Sciences and Systems (CISS)*. 2025, pp. 1–6. DOI: 10.1109/CISS64860.2025.10944698.
- [25] Su Hang and Wei Li. “OTFS for Underwater Acoustic Communications: Practical System Design and Channel Estimation”. In: *OCEANS 2022, Hampton Roads*. 2022, pp. 1–7. DOI: 10.1109/OCEANS47191.2022.9977069.
- [26] Xing Zhang et al. “OTFS-Based Underwater Acoustic Communication System: Modeling and Channel Estimation”. In: *IEEE Transactions on Wireless Communications* (2025), pp. 1–1. DOI: 10.1109/TWC.2025.3606582.
- [27] Guang Yang et al. “Belief-Propagation-Based Low-Complexity Channel Estimation and Detection for

- Underwater Acoustic Communications With Moving Transceivers". In: *IEEE Journal of Oceanic Engineering* 47.4 (2022), pp. 1246–1263. DOI: 10.1109/JOE.2022.3148567.
- [28] Xiaoyu Yang et al. "Research and Implementation on a Real-Time OSDM MODEM for Underwater Acoustic Communications". In: *IEEE Sensors Journal* 23.16 (2023), pp. 18434–18448. DOI: 10.1109/JSEN.2023.3291082.
- [29] Minsung Kim, Davide Venturelli, and Kyle Jamieson. "Leveraging quantum annealing for large MIMO processing in centralized radio access networks". In: *Proceedings of the ACM Special Interest Group on Data Communication. SIGCOMM '19*. Beijing, China: Association for Computing Machinery, 2019, pp. 241–255. ISBN: 9781450359566. DOI: 10.1145/3341302.3342072. URL: <https://doi.org/10.1145/3341302.3342072>.
- [30] Minsung Kim et al. *X-ResQ: Reverse Annealing for Quantum MIMO Detection with Flexible Parallelism*. 2024. arXiv: 2402.18778 [cs.NI]. URL: <https://arxiv.org/abs/2402.18778>.
- [31] Minsung Kim et al. "Physics-inspired heuristics for soft MIMO detection in 5G new radio and beyond". In: *Proceedings of the 27th Annual International Conference on Mobile Computing and Networking. MobiCom '21*. New Orleans, Louisiana: Association for Computing Machinery, 2021, pp. 42–55. ISBN: 9781450383424. DOI: 10.1145/3447993.3448619. URL: <https://doi.org/10.1145/3447993.3448619>.